

Influence of digitisation on master–slave synchronisation in chaos-encrypted data transmission

X. Bavard, A. Locquet, L. Larger and J.-P. Goedgebuer

Abstract: The impact of digitisation on chaos synchronisation and message decoding in a chaotic cryptosystem is described. The sampling rates and resolutions that lead to a good decoding of the message are determined numerically and experimentally. The results are interpreted in light of Shannon’s sampling theory.

1 Introduction

The properties of chaotic systems can be exploited to realise secure communications. The noise-like appearance of chaos and its broadband spectrum can be used to hide an information-bearing message. Decoding of the message at the receiver is made possible through chaos synchronisation with the emitter. Chaotic communications have been realised with electronic circuits [1–4], and with optical devices using solid-state Nd:YAG lasers [5], erbium-doped fibre lasers [6–10] and semiconductor lasers [11–24].

Most of these encrypted transmissions have been performed so far with carriers that are analogue chaotic signals. It is interesting to realise chaotic communications that take advantage of the unique features of digital communications, such as their low sensitivity to noise and the existence of a wealth of digital modulation formats. One approach towards this is to use a physical system which produces digital chaos. For example, Larger *et al.* [25] have recently demonstrated a generator of optical pulses, whose intensity varies chaotically. In this article, we investigate another approach that consists of digitising the transmitted signal, formed by the message masked by chaos, in order to take advantage of the resistance of digital transmission formats to channel impairments. The results obtained with a nonlinear delayed feedback generator of wavelength chaos [26], which is known to produce high-dimensional chaos, has been reported. The influence of the distortions induced by the sampling and quantisation processes on chaos synchronisation and message decoding have been examined. Numerical simulations are presented and compared with experimental results for different parameters of the digital conversion.

2 Principle

A schematic diagram of the cryptosystem under consideration is shown in Fig. 1. The chaotic transmitter is formed by a wavelength-tuneable diode laser (DBR) at 1.55 μm , with a feedback loop containing a nonlinear element NL made of a birefringent plate (BP) set between two crossed polarisers, a photodetector PD, a laser diode (LD), a delay line introducing a time delay T , an amplifier with gain β (the feedback strength), and a first-order low-pass filter with a 20 kHz cut-off frequency. We refer the reader to Larger *et al.* [26] for a complete description of this system, which was originally used for analogue transmissions [11, 12].

The dynamics of this assembly is ruled by a delay-differential nonlinear equation [11]

$$x(t) + \tau \frac{dx(t)}{dt} = \beta\{\text{NL}[x(t - T)] + s(t)\} \quad (1)$$

where $x(t)$ denotes the chaotic dynamical variable, which is related to the wavelength deviation $\lambda(t)$ from the central wavelength Λ_0 emitted by the laser diode, τ is the time constant of the filter, NL is the nonlinear function, β is the feedback strength and $s(t)$ is the message to be encrypted. The wavelength $\lambda(t)$ obeys (1) with

$$x(t) = \frac{\pi D}{\Lambda_0^2} \lambda(t), \quad \beta = \frac{\pi D}{\Lambda_0^2} \beta_\lambda$$
$$\text{NL}[x(t - T)] = \sin^2[x(t - T) + \phi], \quad \phi = \frac{\pi D}{\Lambda_0} \quad (2)$$

where D is the optical path-difference of BP, β_λ the feedback strength in λ units and ϕ is a phase shift.

The message is introduced in the feedback loop and thus participates actively to the dynamics, as shown by (1). The open-loop receiver is a replica of the transmitter (in the sense that it is formed by the same elements). The dynamical variable x propagates towards the receiver and is coupled into it. The dynamics of the receiver system is described by the following delay-differential equation

$$y(t) + \tau \frac{dy(t)}{dt} = \beta \text{NL}[x(t - T_c)] \quad (3)$$

where T_c is the propagation time between the transmitter and the receiver. The parameter mismatches, the presence

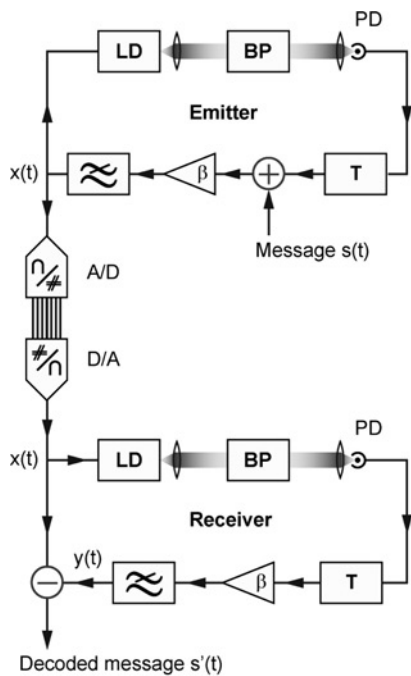


Fig. 1 Schematic diagram of digital transmission between the emitter and the receiver

of noise in the cryptosystem and channel-induced distortions, which all degrade the quality of the decoding and synchronisation processes have been neglected [23, 27]. It is easy to show that, in the absence of message, $y(t)$ synchronises perfectly with $x(t - T_c + T)$. This is a form of anticipating synchronisation [22] as the receiver dynamical variable y synchronises at time t with the emitter signal that will be coupled into it T seconds later. In the presence of a message $s(t)$, the difference $\Delta(t) = x(t - T_c + T) - y(t)$ follows the following first-order non-autonomous differential equation

$$\Delta(t) + \tau \frac{d\Delta(t)}{dt} = \beta s(t)$$

Therefore the difference between the emitter and receiver variables, taken with the correct time lag, gives the information-bearing message, multiplied by a factor β , and filtered by a first-order filter of cut-off frequency $1/(2\pi\tau)$. In this method, chaos is used as a masking signal, and the encryption and decryption processes are essentially analogue.

At both ends of the transmission channel, a pair of analogue–digital (A/D) and digital–analogue (D/A) converters is inserted (Fig. 1). The process of digitisation includes three basic steps: sampling, quantising and coding. Sampling corresponds to the discretisation of time applied to an analogue signal. Once the sampled signal is obtained, it is quantified by rounding off its value to the closest value of the converter scale. Finally, coding is carried out: it associates each output value to a binary word. D/A conversion is essentially the reverse process. The D/A converter produces a staircase-like signal, according to the pre-established code, which is then smoothed by a filter.

3 Numerical results

The influence of signal digitisation was first studied through numerical simulations. The following parameter values were used for the transmitter and receiver systems:

$\Lambda_0 = 1.55 \mu\text{m}$, $T = 512 \mu\text{s}$, $\beta_\lambda = 500 \text{ pm}$, $D = 22 \text{ mm}$ and the cut-off frequency of the low-pass filter was $f_c = 20 \text{ kHz}$, leading to a response time τ of $8 \mu\text{s}$. These parameter values lead to fully developed chaos of large dimension and entropy. We used two types of information-bearing message: a sinusoidal signal and a realistic broadband voice signal. The digitisation of the composite transmitted signal, formed by the chaotic carrier and the encrypted message, was simulated numerically for various quantisations (10–24 bit) and different sampling rates f_s (40–1000 kHz). Fig. 2 shows the decoded message, $s'(t) = x(t) - y(t)$, for three values of the resolution (10, 12 and 24 bit) and three values of the sampling rate (80, 176 and 192 kHz), when a 500 Hz sinusoidal signal $s(t)$ of amplitude 0.04 is used as a message. It can be seen that the decoding quality depends heavily on the resolution and on the sampling frequency. Below a threshold frequency of approximately 180 kHz, it is impossible to recover the message, whatever the resolution is. We see, for example, that for a sampling frequency of 80 kHz, the signal-to-noise ratio (SNR) does not exceed 7 dB, even for a resolution of 24 bit. At the threshold sampling rate, a resolution of 10 bit leads to an SNR of 20 dB and to a sinusoidal message that is distinguishable in the decoded message $s'(t)$. The original message $s(t)$ can be recovered by filtering $s'(t)$. This value of 20 dB will be used as a reference value to compare different system configurations. Above the threshold sampling frequency, it is always possible to recover the message. In addition, we note that an increase of f_s for a given resolution, or an increase of the resolution for a given f_s , leads to an increase of the SNR.

The degradation of the quality of the decoded message in the digital transmission is due to the distortions induced by the sampling and quantisation processes, which degrade the quality of the synchronisation. Ideally, the sampling rate should be at least two times bigger than the maximum frequency of the chaotic spectrum (Shannon criterion) to avoid aliasing. The spectrum of the generated chaos is shaped by the in-loop filter, and thus roughly exhibits the same frequency dependence. As it is a first-order filter, a significant part of the chaotic spectrum is located at frequencies higher than 20 kHz, as shown in Fig. 3. Because of the wideband

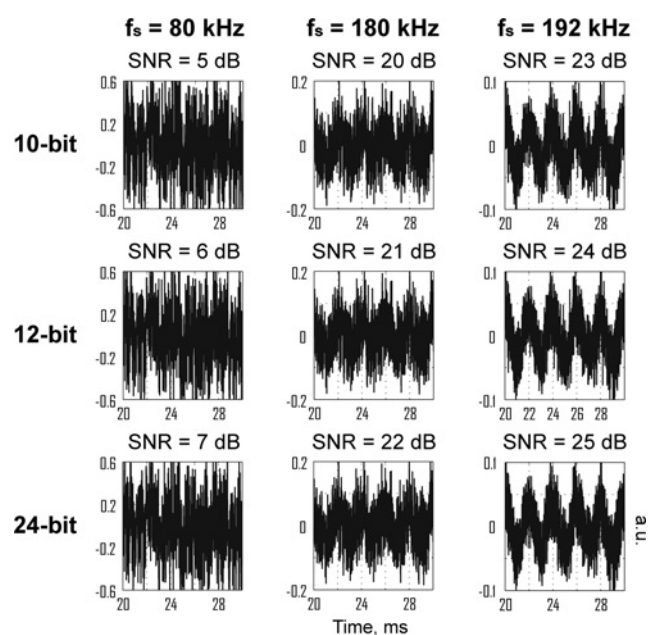


Fig. 2 Decoded message for different values of the sampling frequency and of the resolution (in bit) of the quantisation

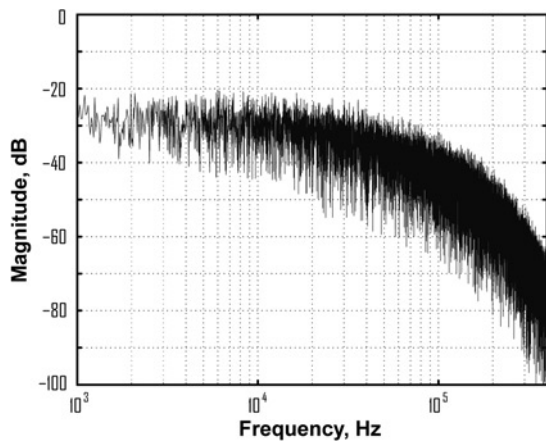


Fig. 3 Spectrum of the chaotic signal $x(t)$ produced by the emitter (1), in presence of a sinusoidal message $s(t)$ of amplitude 0.04 and frequency 500 Hz

nature of the spectrum, it is necessary to use very large sampling rates to meet the Shannon criterion. It is interesting to determine the highest significant frequency of the spectrum that has to be taken into account to obtain good synchronisation and decoding qualities. We consider for this the setup represented in Fig. 4, in which an ideal low-pass filter, which can be considered as an ideal anti-aliasing filter, is placed between the emitter and the receiver systems. This ideal filter completely removes all the frequency components above its cut-off frequency f_c . The decoded message $s'(t)$ is represented in Fig. 5 for various cut-off frequencies. We observe that for cut-off frequencies f_c greater than 90 kHz, the SNR is greater than 20 dB, and the message can be decoded. This means that the portion of the chaotic spectrum above 90 kHz, approximately, can be neglected as it is not necessary for the synchronisation and decoding processes. The results of Fig. 2 can be analysed in light of these observations. If the sampling rate f_s is larger than the threshold value of $2 \times 90 = 180$ kHz, the aliasing that results is limited and the message can be decoded. When the sampling frequency is smaller than the threshold value, the distortion induced by the aliasing is too strong to allow a good decoding of the message, even in the absence of quantisation. The quantisation of the

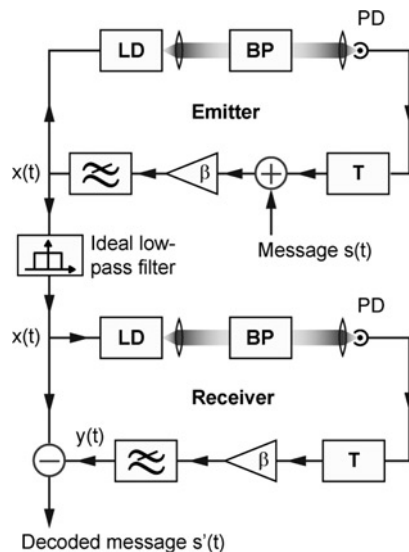


Fig. 4 Schematic diagram with an ideal filter between the emitter and the receiver

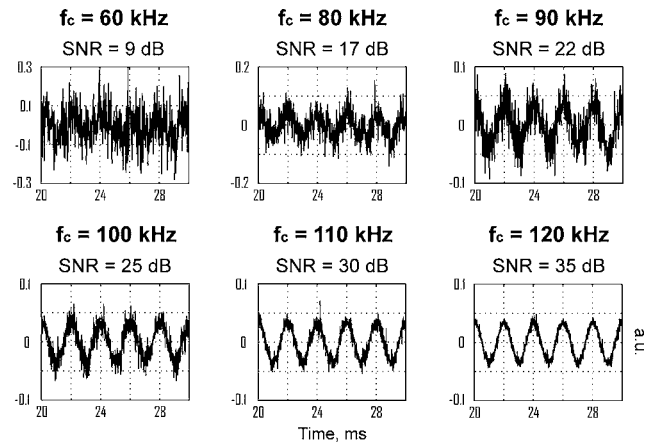


Fig. 5 Evolution of decoding quality as a function of the cut-off frequency f_c of an ideal low-pass filter

chaotic signal can only degrade further the quality of the synchronisation and decoding processes, as can be seen from Fig. 2. The finer the resolution of the quantisation, the smaller the distortions of the chaotic signal, and therefore the better the synchronisation and decoding qualities. Because only relatively large resolutions have been considered in Fig. 2, the SNR are seen to increase only moderately with the resolution. In addition, it should be noted that the amplitude of the message considered here (0.04) is such that it provides simultaneously security and sufficient decoding quality. Amplitudes that are significantly larger would lead to a message frequency that is easily identifiable in the spectrum of the transmitted signal. Smaller amplitudes would lead to a decrease of the SNR because the degradation of the quality of the synchronisation, and thus of the decoded message, is almost independent of the amplitude of this message.

It has been explained earlier that with the first-order cryptosystem described by (1), a sampling frequency larger than 180 kHz is necessary to transmit a 500-Hz sinusoidal message. The biggest part of the chaotic spectrum is necessary for the synchronisation, but is not used to hide the information-bearing message. The same phenomenon is found for digital messages. It thus appears that the first-order system is not very spectrally efficient. By this we mean that it requires a large spectrum and a large sampling frequency, compared to the message spectral width.

We have decided to investigate a new system which produces a more limited chaotic spectrum. The new chaotic emitter is similar to the one described by (1), except for the fact that the first-order RC filter is replaced by an eighth-order Butterworth filter, with the same cut-off frequency as in the case of the first-order filter ($f_c = 20$ kHz). The emitter can be modelled by the following delay-differential equation

$$x(t) + \sum_{i=1}^8 \alpha_i \frac{d^i x(t)}{dt^i} = \beta \{NL[x(t-T)] + s(t)\} \quad (4)$$

where α_i are the filter coefficients. The receiver system also uses an eighth-order system and its dynamical behaviour is described by

$$y(t) + \sum_{i=1}^8 \alpha_i \frac{d^i y(t)}{dt^i} = \beta NL[x(t-T)] \quad (5)$$

With an eighth-order filter, the frequencies in the chaotic spectrum that are above the cut-off frequency experience a much stronger attenuation than with a first-order system, as

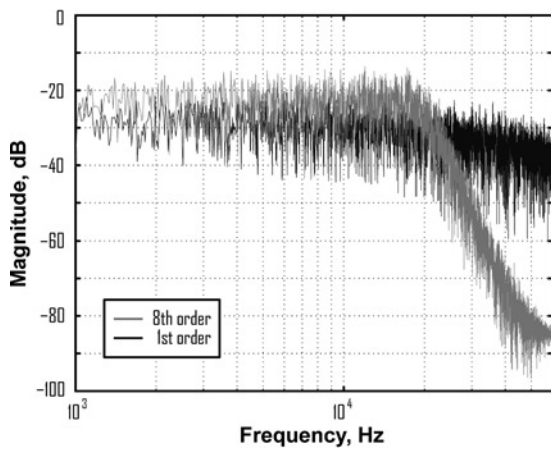


Fig. 6 Spectra of the chaotic signals $x(t)$ produced by the first- (black) and eighth- (grey) order cryptosystems

is confirmed by Fig. 6, which represents the spectrum of the chaotic signal x produced by the first- and eighth-order filters.

The evolution of the SNR of the decoded message, as a function of the sampling frequency, is represented in Fig. 7, for a first-order and an eighth-order filter. The form of the curves is similar for the two cases. For increasing sampling frequencies, we observe that the SNR curves are first identical for different quantisations, then they separate and finally, for large sampling frequencies, the SNR becomes independent of the sampling frequency. When the curves are superimposed, the degradation in the synchronisation quality because of the aliasing is so strong that the influence of the number of bits in the quantisation is not significant. The curves separate when the degradation induced by the aliasing becomes of the same order of magnitude as the degradation induced by the quantisation. When the curves become horizontal, the sampling frequency is large enough for no aliasing to occur, and the SNR is dictated by the number of bits in the quantisation only.

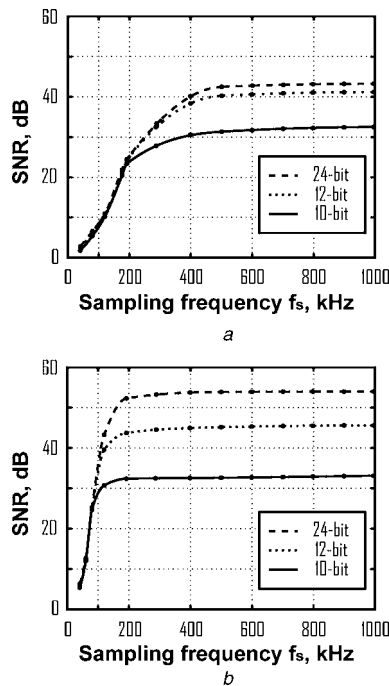


Fig. 7 Numerical SNR with two different intraloop filters

- a First-order filter
- b Eighth-order filter

A marked difference between the behaviours of the first- and eighth-order cases is that the SNR curves increase much more rapidly with the sampling frequency in the latter case. This is because of the smaller bandwidth of the chaotic signal generated by the eighth-order emitter, which requires smaller sampling frequencies to make the aliasing phenomenon negligible. For example, if we consider the reference SNR of 20 dB, we observe that it corresponds to a sampling frequency of 80 kHz in the eighth-order case, whereas a significantly larger frequency of 180 kHz is necessary with the first-order filter. These results confirm that the eighth-order cryptosystem has a better spectral efficiency than the first-order system. Another way of increasing this efficiency could be to multiplex several information-bearing messages, by using, for example, the phenomenon of dual synchronisation [28]. We have checked that the result presented in this section holds for message frequencies ranging from a few tens of Hz to 20 kHz.

Next, we endeavour to answer the following question. Given a transmission channel at a fixed bit rate, what combination of sampling frequency and resolution is optimal in terms of synchronisation? Fig. 8 shows the SNR at the receiver as a function of these two parameters for the eighth-order filter. The dotted lines represent iso-bit-rate curves, where the bit rate is considered to be the product of the sampling frequency with the number of bits of the quantisation. We observe that for a bit rate of 1 Mbit/s, the best SNR is obtained for the largest sampling frequency, because spectral aliasing is the dominant phenomenon. For a bit rate of 2 Mbit/s, the maximal SNR is obtained for a sampling frequency of 143 kHz and a resolution of 14 bit. This maximum corresponds to a trade-off between the degradations induced by the sampling and quantisation processes, leading to the best possible synchronisation and decoding quality. The same type of behaviour is observed for a bit rate of 3 Mbit/s. For bit rates above 4 Mbit/s, the best SNR is obtained for the smallest sampling frequency, and therefore for the largest number of bits. This is due to the fact that the sampling frequencies considered in the graph are sufficiently large to prevent spectral aliasing to take place. The best decoding will thus be obtained with the finest quantisation, and therefore with the smallest sampling frequency.

4 Experimental results

We have tested experimentally the transmission of a sinusoidal message using the cryptosystem represented in

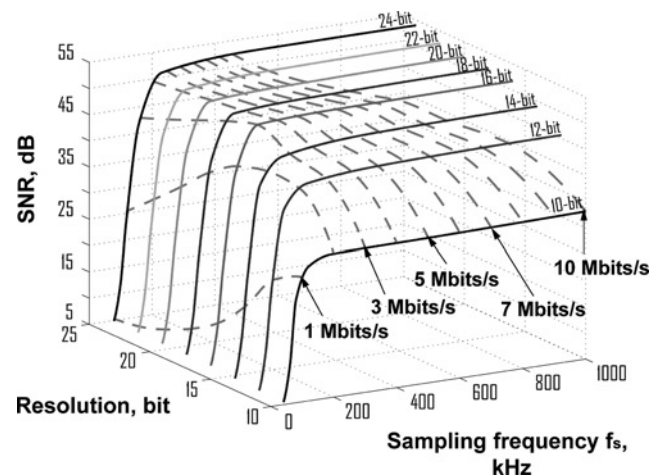


Fig. 8 SNR as a function of resolution and sampling rate

Dotted lines are iso-bit-rate curves

Fig. 1. Fig. 9a represents the synchronisation diagram of the master and slave chaotic signals in the case of the eighth-order filter and of a 12-bit converter at 500 kHz. The message to be encoded is the 500 Hz sinusoidal signal represented in Fig. 9b, while Figs. 9c and d are plots of the encrypted and decrypted signals. The SNR at the receiver output is found to be 26.6 dB. The decoding error can be due to the quantisation and sampling processes, to a mismatch between the parameters of the transmitter and the receiver, and to the presence of noise in the cryptosystem. The SNR obtained from numerical simulations with perfectly matched parameters, in the absence of noise and conversions, is of 29.7 dB. Experimentally, in the absence of converters, the SNR is found to be 28.8 dB, which indicates that a degradation of 0.9 dB is induced by the noise and parameter mismatch. An additional degradation of 2.2 dB is caused by the sampling and quantisation processes.

To investigate systematically the effect of sampling and quantisation, we used three pairs of converters with different resolution: 10, 12 and 24 bit. Also, for each resolution, the sampling rate was varied between 48 kHz and 1 MHz. The converters used are a Burr-Brown ADS803 A/D converter and an Analog Devices AD9752 D/A converter for the 10- and 12-bit resolutions, and an Ego Systems Waveterminal 192× sound card for the 24-bit resolution. The other components used in the experimental setup are described by Larger *et al.* [26]. Figs. 10a and b represent the SNR as a function of the sampling frequency and of the number of bits in the quantisation, for the first-order and eighth-order low-pass filters, respectively.

The evolution of the SNR is similar to the evolution determined numerically (Fig. 7). We find that, first, when there is a strong spectral aliasing, the SNR curves are identical for different resolutions, then these curves split

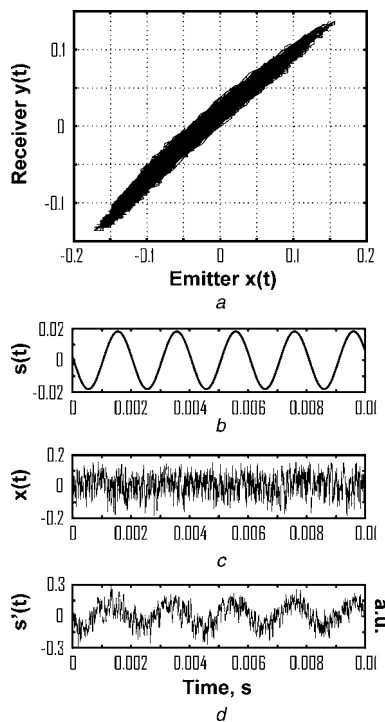


Fig. 9 Experimental digital transmission using a pair of 12-bit converters with a 500-kHz sampling rate

- a Master-slave synchronisation diagram
- b Original message
- c Encrypted signal
- d Decrypted message

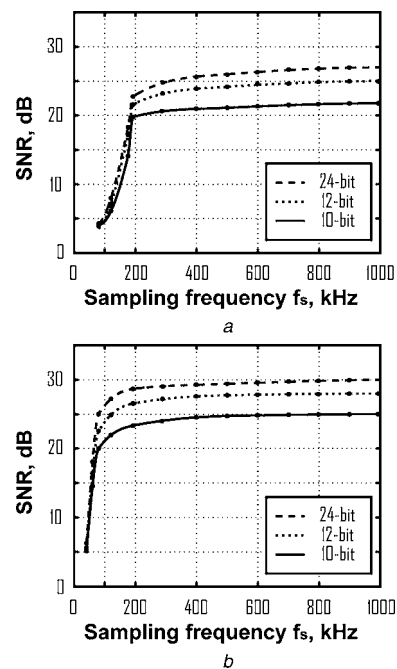


Fig. 10 Experimental SNR with two different intraloop filters

- a First-order filter
- b Eighth-order filter

depending on the resolution and finally, they become independent of the sampling, when the aliasing phenomenon is negligible. Fig. 10 also shows that the reference SNR of 20 dB is reached for values of the sampling frequency that are close to the ones found numerically (80 and 200 kHz, approximately, for the first- and eighth-order filters, respectively). More generally, we observe that the qualitative changes in the shapes of the SNR curves occur for similar values on the numerical and experimental plots. This means that the sampling frequency ranges in which either the sampling or quantisation processes are dominant are also similar. The main difference between the experimental and numerical results is that the SNR values reached for large sampling rates, when the effect of quantisation is dominant, are significantly lower in the case of the experimental results. This difference can be attributed to parameter mismatches and to experimental noise.

We have verified experimentally that the results hold for sinusoidal signals with frequencies ranging from 500 Hz to 20 kHz, as well as for a broadband voice signal.

5 Conclusions

The impact of digitisation of the chaotic waveform on the synchronisation and decoding properties of chaotic cryptosystems are studied numerically and experimentally. We have determined the influence of the sampling rate, and of the resolution of the quantisation, on synchronisation and message recovery, depending on the configuration of the cryptosystem, and on the desired bit rate. In particular, we have brought to light the existence of a threshold sampling frequency, below which it is impossible to obtain synchronisation, independently of the quality of the quantisation. It appears that this minimum sampling frequency can be very large with respect to the frequency of the information-bearing message, because the synchronisation process needs almost all the frequencies of the wideband chaotic spectrum. This reveals the low spectral efficiency of

chaotic communications. We show that this efficiency can be increased by using higher-order filters in the chaotic emitter and receiver.

6 References

- 1 Pecora, L.M., and Carroll, T.L.: 'Synchronization in chaotic systems', *Phys. Rev. Lett.*, 1990, **64**, (8), pp. 821–824
- 2 Cuomo, K.M., and Oppenheim, A.V.: 'Circuit implementation of synchronized chaos with applications to communications', *Phys. Rev. Lett.*, 1993, **71**, (1), pp. 65–68
- 3 Voss, H.U.: 'Real-time anticipation of chaotic states of an electronic circuit', *Int. J. Bifurcation Chaos*, 2002, **12**, (7), pp. 1619–1625
- 4 Larger, L., Goedgebuer, J.-P., Udaltsov, V.S., and Rhodes, W.T.: 'Radio transmission system using FM high dimensional chaotic oscillator', *Electron. Lett.*, 2001, **37**, (9), pp. 594–595
- 5 Colet, P., and Roy, R.: 'Digital communication with synchronized chaotic lasers', *Opt. Lett.*, 1994, **19**, (24), pp. 2056–2058
- 6 VanWiggeren, G.D., and Roy, R.: 'Communication with chaotic lasers', *Science*, 1998, **279**, (5354), pp. 1198–2000
- 7 VanWiggeren, G.D., and Roy, R.: 'Optical communication with chaotic waveforms', *Phys. Rev. Lett.*, 1998, **81**, (16), pp. 3547–3550
- 8 VanWiggeren, G.D., and Roy, R.: 'Chaotic communication using time-delayed optical systems', *Int. J. Bifurcation Chaos*, 1999, **9**, (11), pp. 2129–2156
- 9 Abarbanel, H.D.I., and Kennel, M.B.: 'Synchronizing high-dimensional chaotic optical ring dynamics', *Phys. Rev. Lett.*, 1998, **80**, (14), pp. 3153–3156
- 10 Luo, L.G., Chu, P.L., and Liu, H.F.: '1-GHz optical communication system using chaos in erbium-doped fiber lasers', *IEEE Photonics Technol. Lett.*, 2000, **12**, (3), pp. 269–271
- 11 Goedgebuer, J.-P., Larger, L., and Porte, H.: 'Optical cryptosystem based on synchronization of hyperchaos generated by a delayed feedback tunable laser diode', *Phys. Rev. Lett.*, 1998, **80**, (10), pp. 2249–2252
- 12 Larger, L., Goedgebuer, J.-P., and Delorme, F.: 'Optical encryption system using hyperchaos generated by an optoelectronic wavelength oscillator', *Phys. Rev. E*, 1998, **57**, (6), pp. 6618–6624
- 13 Sivaprakasam, S., and Shore, K.A.: 'Demonstration of optical synchronization of chaotic external-cavity laser diodes', *Opt. Lett.*, 1999, **24**, (7), pp. 466–468
- 14 Sivaprakasam, S., and Shore, K.A.: 'Signal masking for chaotic optical communication using external-cavity diode lasers', *Opt. Lett.*, 1999, **24**, (17), pp. 1200–1202
- 15 Sivaprakasam, S., and Shore, K.A.: 'Message encoding and decoding using chaotic external-cavity diode lasers', *IEEE J. Quantum Electron.*, 2000, **36**, (1), pp. 35–39
- 16 Heil, T., Mulet, J., Fischer, I., Mirasso, C.R., Peil, M., Colet, P., and Elsässer, W.: 'ON/OFF phase shift keying for chaos-encrypted communication using external-cavity semiconductor lasers', *IEEE J. Quantum Electron.*, 2002, **38**, (9), pp. 1162–1170
- 17 Scirè, A., Mulet, J., Mirasso, C.R., Danckaert, J., and Miguel, M.S.: 'Polarization message encoding through vectorial chaos synchronization in vertical-cavity surface-emitting lasers', *Phys. Rev. Lett.*, 2003, **90**, (11), p. 113901-1–113901-4
- 18 Lee, M.W., Rees, P., Shore, K.A., Ortin, S., Pesquera, L., and Valle, A.: 'Dynamical characterisation of laser diode subject to double optical feedback for chaotic optical communications', *IEE Proc., Optoelectron.*, 2005, **152**, (2), pp. 97–102
- 19 Liu, J.-M., Chen, H.-F., and Tang, S.: 'Synchronized chaotic optical communications at high bit rates', *IEEE J. Quantum Electron.*, 2002, **38**, (9), pp. 1184–1196
- 20 Liu, Y., Davis, P., Takiguchi, Y., Aida, T., Saito, S., and Liu, J.-M.: 'Injection locking and synchronization of periodic and chaotic signals in semiconductor lasers', *IEEE J. Quantum Electron.*, 2003, **39**, (2), pp. 269–278
- 21 Ohtsubo, J.: 'Chaos synchronization and chaotic signal masking in semiconductor lasers with optical feedback', *IEEE J. Quantum Electron.*, 2002, **38**, (9), pp. 1141–1154
- 22 Masoller, C.: 'Anticipation in the synchronization of chaotic semiconductor lasers with optical feedback', *Phys. Rev. Lett.*, 2001, **86**, (13), pp. 2782–2785
- 23 Bogris, A., Kanakidis, D., Argyris, A., and Syvridis, D.: 'Performance characterization of a closed-loop chaotic communication system including fiber transmission in dispersion shifted fibers', *IEEE J. Quantum Electron.*, 2004, **40**, (9), pp. 1326–1336
- 24 Locquet, A., Masoller, C., and Mirasso, C.R.: 'Synchronization regimes of optical-feedback-induced chaos in unidirectionally coupled semiconductor lasers', *Phys. Rev. E*, 2002, **65**, (5), pp. 056205-1–056205-12
- 25 Larger, L., Lacourt, P.-A., Poinot, S., and Hanna, M.: 'From flow to map in an experimental high-dimensional electro-optic nonlinear delay oscillator', *Phys. Rev. Lett.*, 2005, **95**, (4), pp. 043903-1–043903-4
- 26 Larger, L., Goedgebuer, J.-P., and Merolla, J.-M.: 'Chaotic oscillator in wavelength: a new setup for investigating differential difference equations describing nonlinear dynamics', *IEEE J. Quantum Electron.*, 1998, **34**, (4), pp. 594–601
- 27 Cuenot, J.-B., Larger, L., Goedgebuer, J.-P., and Rhodes, W.T.: 'Chaos shift keying with an optoelectronic encryption system using chaos in wavelength', *IEEE J. Quantum Electron.*, 2001, **37**, (7), pp. 849–855
- 28 Liu, Y., and Davis, P.: 'Dual synchronization of chaos', *Phys. Rev. E*, 2000, **61**, (13), R2176–R2179